J Low Temp Phys (2011) 162: 710–717
DOI 10.1007/s10909-010-0304-2

Vibronic Transitions of Atomic Bubbles in Condensed ^{4}He

P. Moroshkin · V. Lebedev · A. Weis

Received: 15 June 2010 / Accepted: 16 November 2010 / Published online: 24 November 2010

Abstract Laser spectroscopy of atomic dopants can be used as a tool for the investigation of elementary excitations in quantum fluids and solids. Here we present results of a laser-spectroscopic study of transition-metal (Au, Cu) atoms in liquid and solid ^{4}He. In particular we observe transitions of inner shell electrons that have not been studied before. Such transitions are weakly perturbed by the interaction with the helium matrix and display a characteristic structure composed of a sharp zero-phonon line and a relatively broad phonon wing.

Keywords Matrix-isolation spectroscopy · Impurities · Phonons

1 Introduction

The phonon spectrum is an important characteristic of quantum fluids and solids and for such systems is mostly measured by neutron scattering. However, in conventional solids, optical (including infrared) spectroscopy of dopants is often used to investigate the lattice vibration spectrum [1]. Optical and IR absorption spectroscopy has also been applied to the study of vibronic spectra of various molecules in quantum matrices, such as helium nano droplets [2]. Those studies provided information about the spectrum of elementary excitations in the matrix that is sufficient to distinguish between the superfluid ^{4}He droplets and normal fluid droplets of ^{3}He. There also exists a number of spectroscopic studies (recently reviewed in [3]) of dopants in bulk liquid and solid helium. Most of that work dealt with metal atoms which strongly distort the matrix by forming nanometer-sized cavities called atomic bubbles.

The structure and properties of atomic bubbles are well established via optical and magnetic-resonance spectroscopy. The interaction with the surrounding helium atoms

P. Moroshkin (✉) · V. Lebedev · A. Weis
Department of Physics, University of Fribourg, Fribourg, CH1700, Switzerland
e-mail: peter.moroshkin@unifr.ch

forming the bubble strongly perturbs the valence electron orbitals of the dopant. It results in a large broadening of the observed atomic spectral lines and their shift towards higher energies. Calculations show that the characteristic frequencies of the bubble surface oscillations (breathing, quadrupole, etc.) lie in the range of 10^{11}–10^{12} Hz. However, very little is known about the coupling between the bubble vibration modes and the elementary excitations of the matrix.

The most extensive experimental and theoretical studies [4, 5] of atomic bubbles have been carried out with alkali-metal atoms (Rb, Cs) as dopants. Spectroscopy of coinage metals (Cu, Ag, Au) in superfluid helium was reported as well [6, 7]. Their electronic structure is similar to that of alkali metals with a single valence electron and a $nS_{1/2}$ ground state. One therefore expects the atomic bubble formation around these atoms embedded in condensed He and the effect of the helium environment on the absorption and fluorescence spectra of the valence electrons to be similar to those in the alkali-metal atoms. In addition to the ns valence electron, a coinage-metal atom possesses ten $(n-1)d$ electrons in a closed shell. In condensed helium the inner $(n-1)d$-shell is screened by the outer ns-shell and is therefore expected to be much less perturbed by the interaction with the matrix.

Here we present an experimental spectroscopic study of laser-excited Cu and Au atoms isolated in superfluid, normal fluid and solid ^{4}He. We give a qualitative interpretation of our observations based on the atomic bubble model.

2 Experiment

The experimental setup is described in detail in our earlier publication [3]. The measurements were performed in superfluid, normal fluid and solid ^{4}He in the pressure range of 1–40 bar. The sample was produced in a helium pressure cell immersed in superfluid helium cooled by pumping on the helium bath. Pressurized liquid or solid helium sample is obtained by condensing and then pressurizing helium gas from an external reservoir. The helium host matrix is then doped with copper (gold) atoms by means of laser ablation with a pulsed frequency-doubled Nd:YAG-laser ($\lambda = 532$ nm) focused onto a solid copper (gold) target mounted at the bottom of the cell. The implanted atoms were excited by the third harmonic ($\lambda = 355$ nm) of a second pulsed Nd:YAG laser. Fluorescence light from the sample volume is collected by a lens located in the cryostat and then analyzed by a grating spectrograph with a resolution of 0.1 nm equipped with a CCD camera.

Of all outer-shell transitions of Cu and Au, the strongest laser-induced fluorescence was observed on the $(n+1)^2S_{1/2} - n^2P_{1/2,3/2}$ fine-structure doublets, with $n = 4$ and 6 for Cu and Au, respectively. Two typical spectra obtained in Cu-doped normal fluid helium at low (7 bar) and high (40 bar) helium pressure are shown in Fig. 1(a). In liquid (both superfluid and normal fluid) helium these two lines are particularly strong and dominate the observed fluorescence spectrum. However, in solid He their intensity is much lower and the spectrum is dominated by molecular bands of the Cu_2 dimer and forbidden inner-shell transitions of Cu which will be addressed below.

Figure 1(a) shows that both components of the doublet have nearly Gaussian line shapes and are strongly broadened and blueshifted with respect to the corresponding

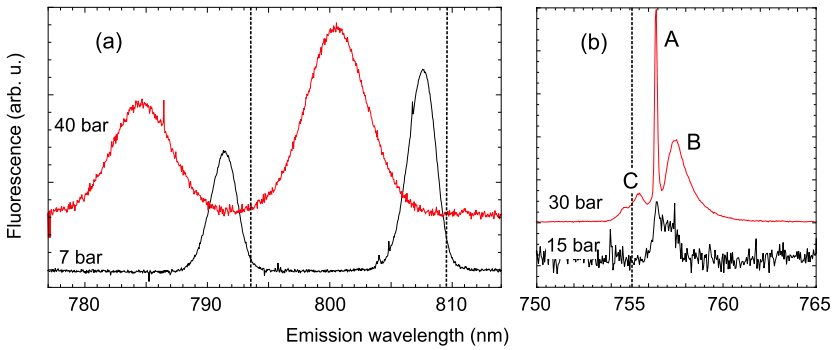

Fig. 1 (Color online) Laser-induced fluorescence spectra of copper atoms in condensed helium. (**a**) $3d^{10}5s\ ^2S_{1/2} - 3d^{10}4p\ ^2P_{1/2,3/2}$ fine-structure doublet; *lower curve*: $T = 2.7$ K, $p = 7$ bar; *upper curve*: $T = 2.6$ K, $p = 40$ bar (normal fluid He). (**b**) $3d^9 4s^2\ ^2D_{3/2} - 3d^{10}4s\ ^2S_{1/2}$ forbidden transition; *lower curve*: $T = 1.5$ K, $p = 15$ bar (superfluid He); *upper curve*: $T = 1.5$ K, $p = 30$ bar (hcp solid He). *Vertical dashed lines* show the transition wavelengths in a free Cu atom

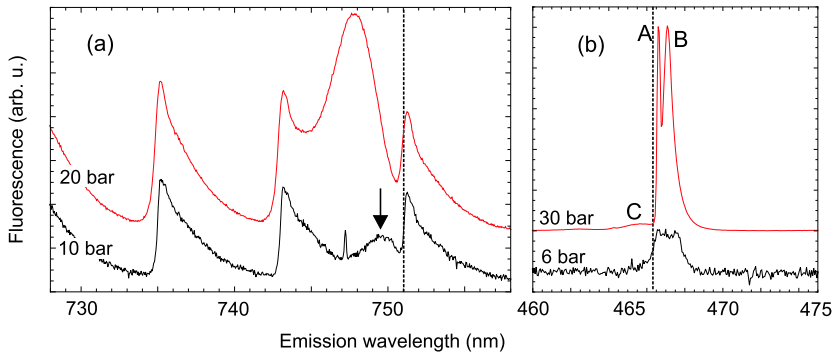

Fig. 2 (Color online) Laser-induced fluorescence spectra of gold atoms in condensed helium. (**a**) $5d^{10}7s\ ^2S_{1/2} - 5d^{10}6p\ ^2P_{3/2}$ line overlapping with a molecular band of Au_2; *lower curve*: $T = 1.5$ K, $p = 10$ bar; *upper curve*: $T = 1.7$ K, $p = 20$ bar (superfluid He). (**b**) $5d^9 6s^2\ ^2D_{3/2} - 5d^{10}6s\ ^2S_{1/2}$ forbidden transition; *lower curve*: $T = 2.7$ K, $p = 6$ bar (normal fluid He); *upper curve*: $T = 1.5$ K, $p = 30$ bar (hcp solid He). *Vertical dashed lines* show the transition wavelengths in a free Au atom

transitions in the free Cu atom. We have studied the pressure dependence of their linewidths and spectral shifts at $T = 1.5$ K and 2.7 K. The former corresponds to the superfluid phase of helium and the latter to the normal fluid. The results obtained in the two phases are nearly identical. The shift δ and the linewidth γ increase linearly with the pressure at rates of $d\delta/dp = 3.3$ cm^{-1}/bar and $d\gamma/dp = 1.8$ cm^{-1}/bar, respectively. The outer-shell transitions of gold (Fig. 2(a)) show a similar behavior.

Besides these valence electron transitions, we have observed laser-induced fluorescence from excited states created by the promotion of an electron from the inner $(n-1)d$ shell to the outer ns orbital. The $(n-1)d^9 ns^2\ ^2D_{3/2,5/2}$ states in free Cu ($n = 4$) and Au ($n = 6$) atoms are metastable and the corresponding transitions towards the $(n-1)d^{10}ns\ ^2S_{1/2}$ ground state are forbidden. Nevertheless, in matrix-

isolated atoms these transitions are usually very strong and dominate the emission spectrum [8, 9]. In Cu-doped condensed helium we have observed lines at 756 nm ($^2D_{3/2} - {}^2S_{1/2}$) and 894 nm ($^2D_{5/2} - {}^2S_{1/2}$), very close to their wavelengths in a free Cu atom. In solid He these lines are much stronger than any of the valence electron transitions or the molecular bands of Cu_2. However, in liquid, and especially in superfluid helium the two lines become much weaker than other spectral features. We attribute this effect to the fact that the diffusion of Cu atoms is much faster in liquid than in solid helium. The decay times of these forbidden transitions are very long ($\simeq$100 ms), so that the excited Cu atoms leave the observation volume faster than they can emit fluorescence. Similar results were obtained in Au-doped helium, where we observe the $^2D_{3/2} - {}^2S_{1/2}$ and $^2D_{3/2} - {}^2D_{5/2}$ transitions at 466 and 815 nm, respectively.

Typical spectra of the $^2D_{3/2} - {}^2S_{1/2}$ transition of Cu obtained in liquid and solid helium are shown in Fig. 1(b). In contrast to the nearly Gaussian $5^2S_{1/2} - 4^2P_{1/2,3/2}$ lineshapes, the $^2D_{3/2} - {}^2S_{1/2}$ transition possesses a very pronounced substructure. In superfluid and normal fluid helium it consists of two overlapping peaks with different widths and heights. The peak on the blue side of the spectrum (labeled A in Fig. 1) is narrower and its spectral width in Fig. 1 is limited by the spectrograph resolution. The second peak (labeled B in Fig. 1) is shifted towards longer wavelength by $\approx$10 cm^{-1} and has a width of $\approx$20 cm^{-1}. Both peaks are present also in solid helium, where the separation between them increases up to $\approx$20 cm^{-1}. In addition to these peaks in solid He there appears another relatively broad feature (labeled C in Fig. 1) on the blue side of the peak A, separated from it by $\approx$20 cm^{-1}. This triplet lineshape remains essentially unchanged within the pressure interval of 28–38 bar in solid He.

All four inner-shell transitions of Cu and Au studied in this work in solid He posses similar characteristic triplet structures. The relative intensities of the triplet components vary significantly from one transition to another. However, their lineshapes plotted on an energy scale are nearly identical. We have investigated the time-dependence of the $^2D_{3/2} - {}^2S_{1/2}$ transition of Cu by varying the delay time between the excitation laser pulse and the CCD exposure time (25 ms). Immediately after the excitation pulse the fluorescence spectrum is dominated by the peak C which disappears completely after the first 25 ms and is replaced by the A plus B doublet. These two peaks decay exponentially with a common decay time $\tau_{AB} = 100 \pm 5$ ms.

3 Discussion

In order to interpret the experimentally observed spectra we assume that Cu and Au atoms in condensed helium reside in nearly spherical atomic bubbles. Unfortunately, potential curves describing the interaction between helium atoms and the excited Cu (Au) atoms are not available. Here, we can therefore only present a qualitative picture of the impurity-bubble interaction. The total energy of the atom + bubble system can be written as [3, 5]:

$$E_{tot} = E_{int} + pV_{bub} + \sigma S_{bub} + \frac{\hbar^2}{8m_{He}} \int \frac{(\nabla \rho(R))^2}{\rho(R)} d^3R + E_{elastic} \qquad (1)$$

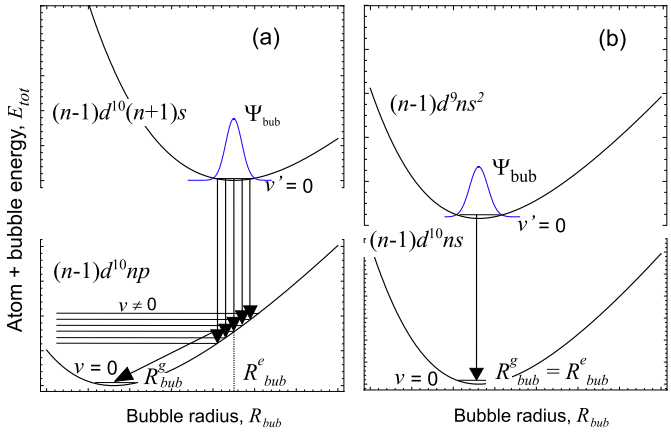

Fig. 3 Potential diagrams of the atom + bubble system: (**a**) electronic transition (fluorescence) in the outer shell accompanied by a large change of the bubble radius; (**b**) electronic transition (fluorescence) in the inner shell without a change of the bubble radius

where p is the helium pressure, σ is the surface tension parameter, V_{bub} and S_{bub} are the volume and the surface area of the bubble, $\rho(R)$ is the helium density profile at the bubble interface, E_{int} is the metal-helium interaction energy, and $E_{elastic}$ is the energy due to the stress created in the solid matrix by the inclusion of the bubble. The same expression without the last term applies also for liquid helium . The interaction term, E_{int} is mostly due to the repulsive interaction of valence electrons of the metal atom with the closed electronic shells of helium atoms at the bubble interface (Pauli repulsion). It rises with the decrease of the bubble radius R_{bub} when the overlap of the electronic densities of Cu (Au) and He increases. The equilibrium bubble size is determined by the balance between E_{int} and the remaining terms in (1) which increase with the bubble radius as R^2_{bub} and R^3_{bub}.

The electronic transitions in the Cu (Au) atom occur at a fixed bubble configuration, as shown schematically in Fig. 3. The transition energy in emission is given by

$$\hbar\omega = \hbar\omega_0 + (E^{(e)}_{int} - E^{(g)}_{int})|_{R_{bub}=R^e_{bub}}, \tag{2}$$

where ω_0 is the transition frequency in the free atom, and the superscripts e and g refer to the electronically excited and the ground state, respectively.

In the frame of the atomic bubble model the lineshape of the fluorescence line is determined by the interaction of the dopant with bubble vibrations [4, 5, 10, 11]. Normally, breathing mode vibrations account for most of the broadening of the spectral line and quadrupolar modes are responsible for its splitting due to the lifting of the M_J degeneracy in the dopant atom (dynamic Jahn-Teller effect). The characteristic frequencies of these vibrations are calculated by solving the one-dimensional Schrödinger equation with a potential energy given by E_{tot} (1) and effective masses $M^{(0)}_{eff} = 4\pi R^3_{bub}\rho m_{He}$ and $M^{(2)}_{eff} = 1/3R^3_{bub}\rho m_{He}$ for the breathing and quadrupolar modes, respectively. The frequencies are of the order of several cm^{-1}. Due to the low temperature of the helium matrix, only the lowest vibration state, $v' = 0$ is populated.

Its wavefunction Ψ_{bub}, also shown in Fig. 3 reflects the delocalization (unsharpness) of the bubble interface.

Let us first consider fluorescence of the $(n+1)^2S_{1/2} - n^2P_{1/2,3/2}$ outer-shell transitions. As shown schematically in Fig. 3(a), the bubble formed around the spherically symmetric excited $(n+1)^2S_{1/2}$ state is large enough to accommodate the $(n+1)s$ electron orbital. The electronic density of the np states has a smaller radial size and fits easily into this large bubble. Its interaction energy is thus much smaller than in the upper electronic state, $E_{int}^{(e)} \gg E_{int}^{(g)}$, which explains the strong blueshift of the transition. The broadening of the fluorescence spectrum is determined by the steepness of the potential curve of the lower state at $R_{bub} = R_{bub}^e$ and by the width of $\Psi_{bub}(R_{bub})$.

The same mechanism is responsible for the shift and broadening of the $n^2P_{1/2} - n^2S_{1/2}$ transitions of alkali-metals Cs and Rb in condensed helium, for which a detailed theoretical analysis is available [3–5]. The electronic density of a Cs atom $(n = 6)$ has its maximum at $R = 2.5$ and 3.4 Å in the ground and excited state, respectively. It results in bubble radii $R_{bub}^g = 5.8$ Å and $R_{bub}^e = 7.4$ Å, and a fluorescence blueshift [5] of $\approx$100 cm^{-1}. Under the same conditions ($T = 1.5$ K, $p = 27$ bar) the $4^2S_{1/2} - 3^2P_{1/2}$ line of Cu is blueshifted by 95 cm^{-1}. Our experiments thus prove the applicability of the atomic bubble model to the defects formed by transition-metal atoms in liquid and solid helium.

As shown in Fig. 3(a), the fluorescence emission occurs in the large bubble and transfers the system into a superposition of highly excited vibration states. The coupling between the bubble vibrations and matrix excitations (phonons) causes a decay of the bubble vibrations towards the state $v = 0$ and stabilizes the bubble interface at a new equilibrium configuration with a smaller radius. A significant part of the bubble energy (dominated by the pV term in (1)) is thus used for the creation of the phonons. A rough estimate of its magnitude can be obtained by noting (Fig. 3(a)) that it has to be larger than the observed spectral width of the transition, $\gamma \approx 30$–100 cm^{-1}, depending on the pressure. This energy is significantly larger than that of a single phonon. We therefore conclude that the outer-shell transition leads to the excitation of a multi-phonon wavepacket in the matrix.

The discussion above applies to the outer-shell electronic transitions which are accompanied by large displacements of the bubble interface. Let us now consider the inner-shell transitions. The corresponding potential diagram is shown schematically in Fig. 3(b). The interaction between the bubble and the metastable $(n-1)d^9ns^2$ metal atom is mostly due to the spherically symmetric ns electronic shell and therefore is very similar to that of the $(n-1)d^{10}ns$ ground state. The transition from the metastable state to the ground state is therefore practically not shifted, $E_{int}^{(e)} - E_{int}^{(g)} \approx 0$, since the transition leaves the bubble radius nearly unchanged, $R_{bub}^g \approx R_{bub}^e$. Instead of a large wave packet, only a few phonons will be excited. There exists also a significant probability of a transition without excitation of a phonon. Such transitions can be observed as a sharp peak in the fluorescence spectrum, very close to the unperturbed transition frequency, and is usually called a zero-phonon line (ZPL). The transitions that excite one or several phonons appear in the fluorescence spectrum as a relatively broad feature called the phonon wing (PW), that is *red-shifted* with respect to the ZPL. In the past, observations of ZPL and PW have been reported in studies of inner-shell transitions of rare-earth elements thulium and europium in liquid and

solid He matrices [12, 13], as well as in the spectra of several molecules attached to He nano droplets [2, 14]. We therefore interpret the peaks A and B (Figs. 1(b) and 2(b)) found in the spectra of the inner-shell transitions of Cu and Au as a zero-phonon line and a phonon wing, respectively.

The origin of the third component of the triplet (peak C) is less clear. The electronic transition may also be accompanied by absorption of phonons from the crystal lattice. Such transitions result in a phonon wing which is *blueshifted* with respect to ZPL. At the temperature of our experiments (1.5 K) only a few thermal phonons are present in the crystal and this second PW should therefore be strongly suppressed. On the other hand, the pulsed laser excitation at 355 nm applied in the present work may locally heat the sample, so that within a short time interval after each laser pulse a significant number of phonons is present in the sample. The relatively short decay time of the peak C points towards this interpretation. On the other hand, it remains unclear, why this spectral feature is missing, or at least strongly suppressed in both liquid phases of He. Since the heat conductivity in solid He is higher than in normal fluid, but lower than in superfluid He, heat dissipation is not responsible for this observation.

In our experiments, Cu and Au atoms become excited by laser radiation at $\lambda = 355$ nm via two-photon near-resonant transitions or via a three-photon ionization and subsequent recombination. In both scenarios one or more highly excited states are produced, which then decay towards the metastable $(n-1)d^9ns^2\ ^2D_{3/2,5/2}$ states via a cascade of radiative and radiationless transitions releasing an energy of about 4–8 eV into the matrix. This process precedes the fluorescence emission and may lead to the creation of crystalline defects (vacancies) attached to the atomic bubble. We can only speculate that peak C is due to such strongly distorted bubbles and that its decay time is determined by the relaxation of the bubble and the surrounding lattice to their regular state. In the liquid phases this relaxation should be much faster than in solid He.

An important aspect of the present work is the comparison of the spectra obtained in different phases of condensed helium: normal fluid, superfluid and hcp solid. Superfluidity plays no role in the formulation of the atomic bubble model. However, all experiments and theoretical calculations up to date were carried out only with dopants in the superfluid phase of helium. It is therefore important to compare data obtained in the superfluid and in the normal fluid phase. The observed lineshapes and shifts of the outer-shell transitions are the same in both phases. Moreover, the spectra obtained in solid He show only a slightly stronger broadening and blueshift than those in liquid He, which can be attributed to the higher helium density. We therefore conclude that superfluidity has no significant effect on the atomic bubble configuration. On the other hand, the spectra of the inner-shell transitions are markedly different in the solid and liquid phases. The behavior of the feature C is discussed above. The phonon wing B changes its shape and in particular the separation between its maximum and the ZPL increases from 10 to 20 cm^{-1}, when going from liquid to solid He. An energy gap of ≈ 6 cm^{-1} between the ZPL and the PW observed in the experiments with He nanodroplets [14], was interpreted as a signature of superfluidity of the droplet. Our spectra obtained in normal fluid He indeed do not exhibit such a gap. No gap was also found in superfluid He, however, in that case the signal to noise

ratio is rather poor. The spectral contour of the PW is determined by the profile of the phonon density of states and by the coupling between the bubble interface vibrations and the phonons. Since the metal-helium interaction does not depend on the state of the matrix, the different shape of the PW in solid and liquid He should be attributed to differences in the phonon spectra.

In summary, we have presented a new spectroscopic study of Au and Cu atoms in liquid and solid He. We observe two types of spectral lines corresponding to outer-shell and inner-shell electronic transitions. The former behave similar then the well-studied spectral lines of alkali metal atoms in condensed helium, in agreement with the atomic bubble model. The second group of transitions possesses a characteristic vibronic structure consisting of a zero-phonon line and two phonon wings. The shape and the intensity of the phonon wings strongly depend on the helium pressure and temperature. These spectra may open a new experimental approach for studying elementary excitations (phonons) in condensed helium.

Acknowledgements This work was supported by grant No. 200020-119786 of the Swiss National Science Foundation. We acknowledge stimulating discussions with J.P. Toennies and E.B. Gordon.

References

1. A.S. Barker, A.J. Sievers, Rev. Mod. Phys. **47**, S1 (1975)
2. J.P. Toennies, A.F. Vilesov, Angew. Chem., Int. Ed. **43**, 2622 (2004)
3. P. Moroshkin, A. Hofer, A. Weis, Phys. Rep. **469**, 1 (2008)
4. T. Kinoshita, K. Fukuda, Y. Takahashi, T. Yabuzaki, Phys. Rev. A **52**, 2707 (1995)
5. A. Hofer, P. Moroshkin, S. Ulzega, D. Nettels, R. Müller-Siebert, A. Weis, Phys. Rev. A **76**, 022502 (2007)
6. B. Tabbert, M. Beau, H. Günther, W. Häußler, C. Hönninger, K. Meyer, B. Plagemann, G. zu Putlitz, Z. Phys. B **97**, 425 (1995)
7. J.L. Persson, Q. Hui, Z.J. Jakubek, M. Nakamura, M. Takami, Phys. Rev. Lett. **76**, 1501 (1996)
8. G.A. Ozin, S.A. Mitchell, J. Garcia-Prieto, J. Phys. Chem. **86**, 473 (1982)
9. S. Lecoultre, A. Rydlo, C. Felix, W. Harbich, Eur. Phys. J. D **52**, 187 (2009)
10. T. Kinoshita, K. Fukuda, T. Yabuzaki, Phys. Rev. B **54**, 6600 (1996)
11. Y. Moriwaki, N. Morita, Eur. Phys. J. D **13**, 11 (2001)
12. K. Ishikawa, A. Hatakeyama, K. Gosyono-o, S. Wada, Y. Takahashi, T. Yabuzaki, Phys. Rev. B **56**, 780 (1997)
13. Q. Hui, M. Takami, J. Low Temp. Phys. **119**, 393 (2000)
14. M. Hartmann, F. Mielke, J.P. Toennies, A.F. Vilesov, G. Benedek, Phys. Rev. Lett. **76**, 4560 (1996)